



Cite this: *RSC Adv.*, 2019, 9, 31122

# Selective removal of silver(i) using polymer inclusion membranes containing calixpyrroles†

Anna Nowik-Zajac, Iwona Zawierucha and Cezary Kozłowski \*

This paper discusses the results of studies on the transport of Ag(i) across polymer inclusion membranes (PIMs), derivatives of calixpyrroles with methyl (KP1) and carboxyl (KP2) groups, as ion carriers, *o*-nitrophenyl pentyl ether (*o*-NPPE) as a plasticizer and cellulose triacetate (CTA) as support. The influence of the pH of the source phase, metal concentration, stripping phase as well as carrier and plasticizer concentration on the efficiency of Ag(i) transport through PIM is presented. Long-term experiments with a supported liquid membrane and a plasticizer membrane demonstrate the durability of the studied PIMs. The obtained results indicate that the competitive transport of Cu(ii), Zn(ii), Ag(i) and Cd(ii) from the aqueous nitrate source phase through KP1 and KP2 is an effective separation method for Ag(i) ions. The prepared PIMs were characterized by scanning electron microscopy (SEM), and atomic force microscopy (AFM) techniques.

Received 10th June 2019  
 Accepted 19th September 2019

DOI: 10.1039/c9ra04347k

[rsc.li/rsc-advances](http://rsc.li/rsc-advances)

## 1 Introduction

In strongly industrialized regions, the wastewater contains large amounts of chemical impurities coming from industry. Achieving high removal efficiency of pollutants leading to the reuse of purified water and simultaneous recovery of valuable metals from wastewater requires many complementary technologies.

Up to now various techniques, including chemical precipitation, extraction, ion exchange, membrane separation and sorption, have been developed for the effective removal of metal ions from different aqueous solutions at various concentrations.<sup>1</sup>

In the process of selective recovery and concentration of metal ions from aqueous solutions liquid membranes, and in recent years also polymer inclusion membranes (PIMs) could be an alternative for liquid–liquid extraction procedures.<sup>2</sup> The efficiency and selectivity of PIM depends on the nature of metal ion carrier introduced into membrane. Different metal ions that can be transported from the feed solution to the stripping solution using PIMs containing a number of carriers are listed by Nghiem *et al.*<sup>3</sup> and Almeida *et al.*<sup>4</sup>

PIM potential for the separation of metallic species is due to their characteristic high selectivity and mechanical properties, which can be improved. For example reinforcing the membrane's support material with functional nanomaterials improves the permeability, contamination resistance,

mechanical and thermal stability of the membranes.<sup>5</sup> On the other hand the application of constant electric current in membrane extraction experiments opens a new opportunity for achieving the excellent selectivity and long-term use of polymer inclusion membrane.<sup>6</sup>

The present commercial extractants enable an efficient removal of metal ions but sometime with low selectivity. Therefore PIM researchers are generally interested in macrocyclic and macromolecular compounds due to their excellent separation selectivity.

The complexation ability of these compounds depends on the size of the ligand cavity, on the ionic potential of the cation to be bound, on the spatial localization of donor binding sites of the ligand, on the presence of additional chemical groups and heteroatoms, and on the nature of the used solvent.

Today a main drawback, strongly limiting the practical use of liquid membranes, constitutes their low durability and non-stable work. These are obviously related with the composition of liquid membranes (the kind of the carrier, of organic solvent and of the surfactant) as well as with their structure.<sup>7,8</sup>

Lifetime of liquid membranes is limited by washing the carrier from membrane to aqueous solvents, forming an emulsion on the interface membrane, the progressive wettability of the pores of the polymeric support, pressure differences between the source and receiving phases, blocking of the membrane pores by the formation of sediment on the membrane surface as well as by the appearance of an osmotic pressure gradient on both sides of the membrane.<sup>9</sup>

An important factor determining the possibility of the commercial use of polymer inclusion membranes is the stability of their operation. Although PIMs are considered to be more stable compared to supported liquid membranes (SLM),

*Institute of Chemistry, Health and Food Sciences, Jan Długosz University of Częstochowa, PL42200 Częstochowa, Poland. E-mail: c.kozłowski@ajd.edu.pl; a.zajac@ajd.edu.pl*

† Electronic supplementary information (ESI) available. See DOI: 10.1039/c9ra04347k



washing the carrier and plasticizer or modifier (if present) from organic phase filling PIM matrix pores, which resulted in the reduction of examined metal ions separation, was observed under certain conditions of metal ions transport.<sup>10–12</sup> The loss of the membrane liquid phase, consisting of the carrier and the plasticizer or modifier (if present), could be minimized by increasing the concentration of common anions in the aqueous solution.<sup>13</sup> It should be noted that the much higher stability of PIM (compared to SLM), allows their multiple use.<sup>14</sup>

The literature data devoted to the transport across PIMs applied for the analysis of pharmaceutical, clinical and environmental samples show that these have good long term stability and can be reused up to 30 times without loss of performance.<sup>15–17</sup>

The growing, especially in recent years, interest in macrocycles as potential transporters of metal ions and neutral molecules is a result of their easy synthesis from commercially available reagents, high thermal and chemical stability and selective complexation of ions and neutral molecules. Due to the simple synthesis, often with high yields, and efficient functionalization by substituents that modify their complexing properties, calixpyrroles induce recently a great interest as the selectophores of metal ions. This results also from the fact that in many chemical and biochemical processes the binding of ions plays a key role, therefore compounds able to bind ions are intensively studied.<sup>18</sup>

The demand for highly purified precious metals free from silver contaminations has increased in the electronics industry, which prepares devices using precious metals.<sup>19</sup> Moreover, silver as the most useful noble metal finds numerous applications in other fields such as jewellery, photography, anti-corrosive alloys, *etc.* It is estimated that about 12% of the world's silver resources are used in the production of light-sensitive devices. All over the world, several tons of silver are lost annually in the waste from photographic and galvanizing plants.<sup>20</sup> Since in addition to being a precious metal it is toxic, the separation and recovery of silver from industrial effluents is of a paramount importance.<sup>21</sup>

Nowik-Zajac *et al.*<sup>22</sup> studied the transport of Ag(I) and Cu(II) ions transport across PIMs containing calix[4]pyrrole[2]thiophene as ion carrier and found that the transport Ag(I) ions is faster than Cu(II) ions.

Amiri *et al.*<sup>23,24</sup> showed that the derivatives of the calix[4]pyrroles dissolved in an oil and immobilized on the supported liquid membrane (SLM) based on a polypropylene matrix are effective and selective Ag(I) ion transporters, but do not transport at all Cu(II), Ni(II), Zn(II), Pb(II), Co(II), Cd(II), Cr(III), Fe(II) and Fe(III) ions. The addition of picric acid to the source phase caused shortening of the time of transport process from 3.5 hours<sup>25</sup> to 75 minutes.<sup>24</sup>

The present work deals with the transport of Ag(I) and Cu(II) from nitrate aqueous solutions through PIMs that contain cellulose triacetate or polyvinyl chloride as a support, *o*-nitrophenyl pentyl ether as a plasticizer and calixpyrrole derivatives as ion carriers. We have tested several parameters, such as the concentration of the carrier, the effect of pH in the acceptor phase, and the nature of stripping agents. We have

characterized the membrane with SEM, AFM as well as selectivity and reliability studies.

## 2 Experimental

### 2.1. Chemicals

Inorganic chemicals, *i.e.* silver(I)nitrate, copper(II)nitrate, zinc(II)nitrate, cadmium(II)nitrate, sodium hydroxide, hydrochloric acid, sodium thiosulfate (Na<sub>2</sub>S<sub>2</sub>O<sub>3</sub>), ethylenediaminetetraacetic acid (EDTA) and sodium acetate (CH<sub>3</sub>COONa) were of analytical grade and were purchased from POCh (Gliwice, Poland). Organic reagents, *i.e.* cellulose triacetate (CTA), polyvinyl chloride (PVC, *M<sub>w</sub>* = 40 000–90 000), *o*-nitrophenyl pentyl ether (*o*-NPPE) and dichloromethane were also of analytical grade and were purchased from Fluka and used without further purification. Aqueous solutions were prepared with double distilled water, with a conductivity of 0.1 μS cm<sup>-1</sup>.

### 2.2. Synthesis

The carrier **KP1** was purchased from Aldrich (97.0%, CAS number 4475-42-7, C<sub>28</sub>H<sub>36</sub>N<sub>4</sub>, MW: 428.61). The synthesis of *meso*-tetramethyl-tetrakis-(4-carboxymethylphenoxy)-calix[4]pyrrole (**KP2**) (Fig. 1) was based on the acid catalyzed reaction of pyrrole with ketones.<sup>26</sup> 4-Oxopentanoic acid and pyrrole were dissolved in dry acetone, and cooled to 0 °C. N<sub>2</sub> was bubbled through the mixture for 10 min, next HCl was added dropwise under nitrogen atmosphere. The mixture was stirred at 0 °C for 2 h and then at room temperature overnight. The solvent was removed and a crude product was dissolved in ethyl acetate. The organic phase was washed with water (three times) and dried over Na<sub>2</sub>SO<sub>4</sub>. Chromatographic purification (silica gel, chloroform/methanol: 1/1) yielded **KP2** as a yellow solid (60%). The structure of **KP2** was confirmed from their NMR and elementary analysis. <sup>1</sup>HNMR (Bruker Advance, 300 MHz, acetone-d<sub>6</sub>): δ 11.21 (br, 4H, COOH), 8.81 (br, 4H, NH), 5.69 (br, 8H, pyrrole CH), 2.72 (t, *J* = 6 Hz, 8H, CH<sub>2</sub>), 2.49 (t, *J* = 6 Hz, 8H, CH<sub>2</sub>), 1.51 (br, 12H, CH<sub>3</sub>). Anal. calcd for C<sub>36</sub>H<sub>44</sub>N<sub>4</sub>O<sub>8</sub>: C 65.44, H 6.71, N 8.48. Found: C 64.98, H 6.65, N 8.27.

### 2.3. Preparation of polymer inclusion membranes

Cellulose triacetate (CTA) or polyvinyl chloride (PVC) (as the support), *o*-nitrophenyl pentyl ether (*o*-NPPE) (as the plasticizer), and calix[4]pyrroles **KP1** or **KP2** (Fig. 1) (as the ionic

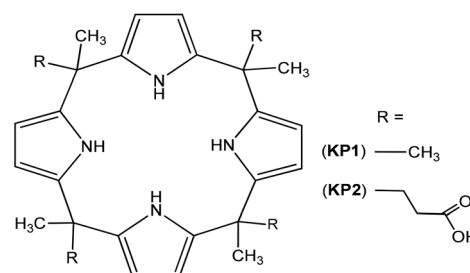


Fig. 1 Structures of calixpyrroles **KP1** and **KP2**.



carrier) were dissolved in dichloromethane. A specified portion of this organic solution was poured on a glass Petri dish consisting of a 5.0 cm glass ring attached to a glass plate with cellulose triacetate – dichloromethane as a glue. Dichloromethane was evaporated overnight and the resulting membrane was separated from the glass plate by immersion in cold water.

#### 2.4. Preparation of supported liquid membranes

The microporous polypropylene membrane Celgard 2500 (Hoechst Celanese) was used as the solid support. This membrane has a porosity of 0.45, a thickness of 0.025 mm, and an effective pore size of 0.040 mm. The membrane was soaked for 12 h in 0.1 M *o*-NPPE solution of the ion carrier.

#### 2.5. Characteristics of PIMs

The thickness of the PIM samples was measured using a digital micrometer (PosiTector 6000 Advance (USA)) with an accuracy of 0.1  $\mu\text{m}$ . The thickness of the membrane was measured 10 times for each case and given as the average value of these measurements, with the standard deviation below 1%. The thickness of membranes before and after transport was found to be the same. The average PIMs thickness varied of 25  $\mu\text{m}$ . Experimental reproducibility was high with standard deviation below 1% of the measured values.

A surface characterization of the polymer membranes was performed using by Atomic Force Microscopy (AFM) (Digital Instruments Veeco Metrology Group). Pores characterization was performed using the AFM image processing program NanoScope v.720 (Digital Instruments Veeco Metrology Group), which enabled the calculation of parameter: roughness ( $R_a$ ). The  $R_a$  parameter is the standard deviation of the  $z$  values within the box cursor and is calculated as:

$$R_a = \frac{1}{N} \sum_{i=1}^N |Z_i| \quad (1)$$

where:  $Z_i$  is the current  $z$  value,  $N$  is the number of points within the box cursors.

A 5 kV scanning electron microscope (SEM) (Quanta 3D FEG, FEI Company) (Hitachi S4500) was used to analyze membrane morphology. Membrane samples were prepared by freezing under liquid nitrogen (70 K) and rapid fracturing, resulting in a clean break fracture image to view the cross-section. The samples were mounted with conductive glue to metal stubs with the fractured edge up and then coated with gold by sputtering. These samples were then viewed in the SEM at around 50  $\mu\text{m}$  magnification.

#### 2.6. Transport studies

Transport experiments were carried out in a permeation cell in which the membrane film (4.9  $\text{cm}^2$  effective surface) was tightly clamped between two compartments.

The composition of the membranes expressed as a weight percentage for **KP1** and **KP2** was as follow: 63–69% plasticizer; 30–30% support; 0.05–7% carrier and 57–67% plasticizer; 27–33% support 0.1–16% carrier, respectively.

The aqueous source phase was a 0.00050 M  $\text{AgNO}_3$  and  $\text{Cu}(\text{NO}_3)_2$ , the aqueous receiving phase was 0.10 M sodium thiosulfate  $\text{Na}_2\text{S}_2\text{O}_3$  (50  $\text{cm}^3$ ). Transport was conducted at a room temperature (23–25  $^\circ\text{C}$ ) and both source and receiving aqueous phases were stirred at 600 rpm with synchronous motors. Samples (0.10  $\text{cm}^3$ ) of an aqueous source phase were removed periodically *via* a sampling port with a syringe and analyzed to determine  $\text{Ag}(\text{I})$  and  $\text{Cu}(\text{II})$  concentration.

The source phase acidity was controlled by pH meter (multi-functional pH meter, CX-731 Elmetron, with combine pH electrode, ERH-136, Hydromet, Poland). Kinetics of transport process through polymer inclusion membrane (PIM) is described by a first-order reaction in respect to metal ion concentration:<sup>20</sup>

$$\ln(c/c_i) = -kt \quad (2)$$

where  $c$  is the metal ion concentration ( $\text{mol dm}^{-3}$ ) in the source phase at a given time,  $c_i$  is the initial  $\text{Ag}(\text{I})$  and  $\text{Cu}(\text{II})$  concentration in the source phase,  $k$  is the rate constant ( $\text{s}^{-1}$ ), and  $t$  is the transport time (s).

To calculate the  $k$  value, a plot of  $\ln(c/c_i)$  versus time was prepared. The rate constant value for the duplicate transport experiment with the averaged standard deviation was calculated. The permeability coefficient ( $P$ ) was calculated as follows:

$$P = (V/A)k \quad (3)$$

where  $V$  is the volume of aqueous source phase, and  $A$  is the area of membrane.

The initial flux ( $J_i$ ) was determined as equal to:

$$J_i = P c_i \quad (4)$$

To describe the efficiency of metal ion removal from the source phase, the recovery factor (RF) was calculated as:

$$\text{RF} = \frac{c_i - c}{c_i} 100\% \quad (5)$$

The metal ion concentrations were measured by flame atomic absorption spectrometry (Solar 939, Unicam). The limits of detection for silver and copper of a flame atomic absorption spectrometry method are: 0.02  $\mu\text{g mL}^{-1}$  and 0.03  $\mu\text{g mL}^{-1}$ , respectively.

The selectivity coefficient  $S$  was defined as the ratio of initial fluxes for M1 and M2 metal ions, respectively.

$$S = J_{i,M1}/J_{i,M2} \quad (6)$$

The reported values correspond to the average of three replicates; the standard deviation observed was within 2%.

## 3 Results and discussion

### 3.1. Kinetics and repeatability of the $\text{Ag}(\text{I})$ transport through polymer inclusion membranes

In order to determine the kinetics and repeatability of the process of  $\text{Ag}(\text{I})$  ions membrane separation through PIM



containing calixpyrroles, the changes of their concentrations in the source and receiving phases as a function of transport time were measured.

The rate of change of concentration of Ag(I) ions in source, receiving phase and the membrane was analyzed for the transport of Ag(I) ions through PIM containing KP2 providing concentration profile of the metal as a function of time.

As seen in Fig. 2, the kinetic curves of  $c/c_i$  relationship in the function of time are of an exponential nature that confirms the kinetic model of metal ions primary transport proposed by Danesi *et al.* in relation to the supported liquid membranes (SLM).<sup>27</sup>

The rate of transport at the border of source phase and membrane, as well as membrane and the receiving phase is comparable, *i.e.* complexation and decomplexation reactions occur with the same rate. Small saturation of the membrane with Ag(I) – KP1 as well as KP2 complex proves the establishing of quasi-stationary state in the membrane phase.

To determine the repeatability of Ag(I) ions transport measurements through PIM containing KP1 and KP2, each experiment was repeated 5 times.

Average constants of transport process ( $k$ ) were estimated, based on the slopes of linear relationship  $\ln(c/c_i) = f(t)$  obtained for applied membrane, and the values of initial fluxes of Ag(I) ions from the source phase ( $J_i$ ) were calculated based on them. The calculation results are presented in Fig. 3. The coefficients of determination ( $r^2$ ) of linear relationships  $\ln(c/c_i)$  in the function of time for KP1 and KP2 carriers amounted to 0.9901 and 0.9115, so the correlations were designated at a high level of significance. Thus, these results are burdened with a relative error not exceeding 1%, and concurrently are calculated at high values of determination coefficients exceeding 0.91. This means that the repeatability of the results of transport through PIM is very good. It can be noticed, taking into account the obtained

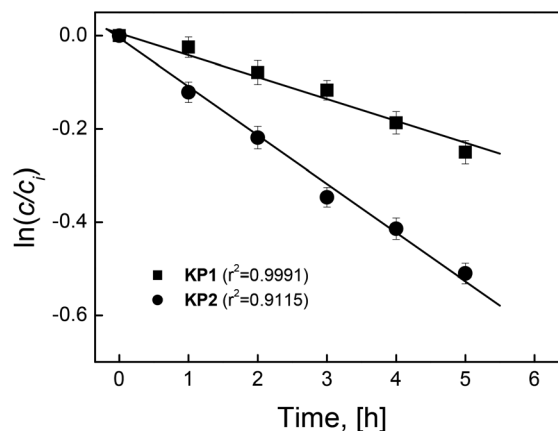


Fig. 3 The relationship  $\ln(c/c_i)$  vs. time transport of ions Ag(I) across PIM with KP1 and KP2. Source phase:  $5.0 \times 10^{-4}$  M AgNO<sub>3</sub>, pH = 4.0; membrane:  $2.0 \text{ cm}^3$  o-NPPE/1.0 g CTA; 0.10 M KP1 and KP2, receiving phase: 0.10 M Na<sub>2</sub>S<sub>2</sub>O<sub>3</sub>. PIMs compositions were 67% plasticizer, 30% support, 3% KP1; and 63% plasticizer, 31% support, 6% KP2.

values of kinetic parameters and their statistical evaluation, that the repeatability of the results is good.

### 3.2. Modification of source phase composition

The effect of source phase acidity within pH range of 2.0–6.0 on Ag(I) ions transport through polymer inclusion membranes was examined as the first. Fig. 4 presents the relationship of initial fluxes of Ag(I) ions transport on pH of the source phase containing  $5.0 \times 10^{-4}$  M AgNO<sub>3</sub> through PIM to the receiving phase containing 0.10 M Na<sub>2</sub>S<sub>2</sub>O<sub>3</sub>.

It turned out that the values of initial fluxes of Ag(I) ions transport increase with an increasing pH from 2.0 to 4.0. For pH = 4.0, the maximum initial fluxes of Ag(I) ions transport from the aqueous source phase containing  $5 \times 10^{-4}$  M AgNO<sub>3</sub> through PIM amounted to  $0.71 \mu\text{mol m}^{-2} \text{ s}^{-1}$  for KP1, and 1.62

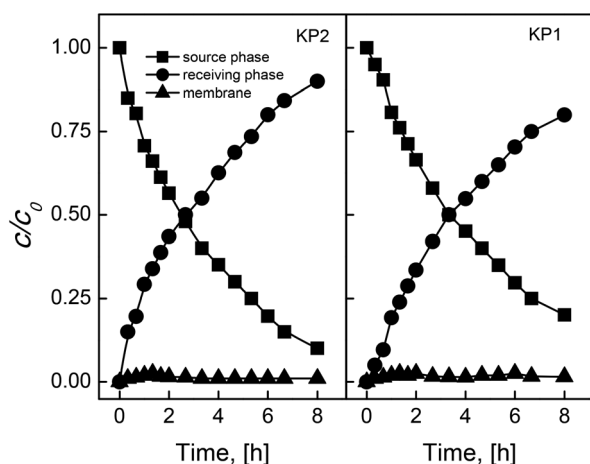


Fig. 2 The profile of Ag(I) concentrations in source, membrane and receiving phases during the transport process across PIMs containing KP1 and KP2. Source phase:  $5.0 \times 10^{-4}$  M AgNO<sub>3</sub>, pH = 4.0; membrane:  $2.0 \text{ cm}^3$  o-NPPE/1.0 g CTA; 0.10 M carrier, receiving phase: 0.10 M Na<sub>2</sub>S<sub>2</sub>O<sub>3</sub>. PIMs compositions were 67% plasticizer, 30% support, 3% KP1; and 63% plasticizer, 31% support, 6% KP2.

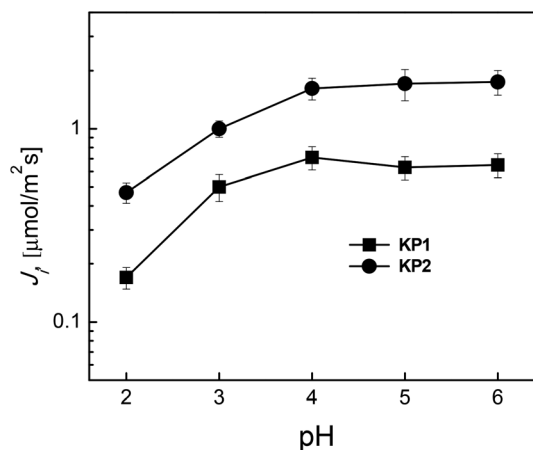


Fig. 4 The relationship of the initial ion flux transport Ag(I) across the PIM vs. the pH of the source phase. Source phase:  $5.0 \times 10^{-4}$  M AgNO<sub>3</sub>; membrane:  $2.0 \text{ cm}^3$  o-NPPE/1.0 g CTA; 0.10 M KP1 and KP2, receiving phase: 0.10 M Na<sub>2</sub>S<sub>2</sub>O<sub>3</sub>. PIMs compositions were 67% plasticizer, 30% support, 3% KP1; and 63% plasticizer, 31% support, 6% KP2.





$\mu\text{mol m}^{-2} \text{s}^{-1}$  for **KP2**. However, in pH range of 4.0–6.0, the transport flux was stabilized at a constant level. The highest increase of  $\text{Ag}(\text{i})$  ions transport rate was observed for **KP2**, which is a carboxyl derivative of calixpyrroles. However, above  $\text{pH} = 4.0$ , the share of carrier particle deprotonation was smaller, hence, small changes in  $J_i$  value were observed for the measurements above  $\text{pH} = 5.0$ . This indicates cooperative transport mechanism, but with greater participation of complexes formation by incorporation the  $\text{Ag}(\text{i})$  ions into the cavity of **KP2**.

Then, an effect of initial  $\text{AgNO}_3$  concentration in the source phase on the rate of transport through PIM was examined. Four  $\text{AgNO}_3$  solutions at  $\text{pH} 4.0$ , containing  $1.0 \times 10^{-4} \text{ M}$ ;  $2.5 \times 10^{-4} \text{ M}$ ;  $5.0 \times 10^{-4} \text{ M}$  and  $1.0 \times 10^{-3} \text{ M}$  of this metal ions were prepared and they were used as the source phases, in order to determine the kinetics of PIM process due to the concentration of  $\text{Ag}(\text{i})$  ions in source phase. The  $0.10 \text{ M Na}_2\text{S}_2\text{O}_3$  solution was used as the receiving phase.

Fig. 5 shows the obtained linear effect of ( $J_i$ ) value on  $\text{Ag}(\text{i})$  concentration in the source phase in log-log arrangement.

The change in the values of  $\text{Ag}(\text{i})$  initial fluxes as a function of metal concentration in the source phase ( $c_i$ ) in a logarithmic arrangement is linear. It indicates that the reactions takes place in the boundary of source phase/membrane involve single  $\text{Ag}(\text{i})$  cation, therefore, this is the first order reaction in respect of a metal ion.

The literature review shows several applications of liquid membranes to real waste solutions treatment. According to the literature<sup>23,28,29</sup> concentration of  $\text{Ag}(\text{i})$  ions in wastewater was between  $4.0\text{--}8.0 \times 10^{-4} \text{ M}$ . Tarahomi *et al.*<sup>28</sup> showed composition of silver plating and photographic waste solution in which silver concentration was  $5 \times 10^{-4} \text{ M}$  at  $\text{pH} 3$ . Amiri *et al.*<sup>23</sup> also showed that the derivatives of the calix[4]pyrroles dissolved in an oil and immobilized to the supported liquid membrane

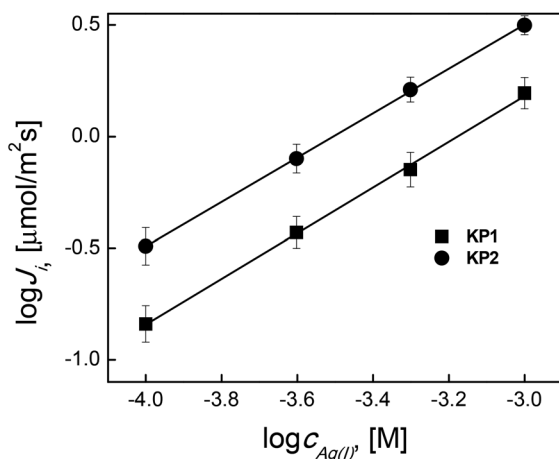


Fig. 5 Logarithmic relation of initial fluxes vs.  $\text{Ag}(\text{i})$  concentration in the source aqueous phase. Source phase: various concentration of  $\text{AgNO}_3$ ,  $\text{pH} = 4.0$ ; membrane:  $2.0 \text{ cm}^3$  *o*-NPPE/ $1.0 \text{ g}$  CTA;  $0.10 \text{ M}$  **KP1** and **KP2**, receiving phase:  $0.10 \text{ M Na}_2\text{S}_2\text{O}_3$ . PIMs compositions were 67% plasticizer, 30% support, 3% **KP1**; and 63% plasticizer, 31% support, 6% **KP2**.

(SLM) based on a polypropylene matrix are effective and selective  $\text{Ag}(\text{i})$  ion transporters. Concentration of  $\text{Ag}(\text{i})$  ions was  $8.0 \times 10^{-4} \text{ M}$ ,  $\text{pH} 4$ . In next experiments, the silver concentration in source aqueous phase was  $1 \times 10^{-3} \text{ M}$  at  $\text{pH} 4$ .

### 3.3. Modification of receiving phase composition

Aqueous solutions of sodium thiosulfate ( $\text{Na}_2\text{S}_2\text{O}_3$ ), ethylenediaminetetraacetic acid (EDTA) and sodium acetate ( $\text{CH}_3\text{COONa}$ ) were used in order to determine the influence of receiving phase on the rate of transport at the boundary of membrane/receiving phase.

Fig. 6 presents the relationship of recovery coefficient (RF) vs. the time of  $\text{Ag}(\text{i})$  transport through PIM containing **KP1** and **KP2**.  $0.10 \text{ M Na}_2\text{S}_2\text{O}_3$ ,  $0.10 \text{ M EDTA}$  as well as  $0.10 \text{ M CH}_3\text{COONa}$  aqueous solutions at  $\text{pH} = 6.0$  were used as the receiving phases.

In the case of membrane system containing calixpyrrole carriers **KP1** and **KP2** the transport of silver ions was effectively followed using sodium thiosulfate as aqueous receiving phase.

The maximum value for the  $\text{Ag}(\text{i})$  recovery factor after 6 hours of transport obtained for **KP2** was  $\text{RF} = 74.5\%$  ( $0.10 \text{ M Na}_2\text{S}_2\text{O}_3$  as the receiving phase). The yield of  $\text{Ag}(\text{i})$  ions separation using the above mentioned receiving phases decreased in the following order:  $\text{Na}_2\text{S}_2\text{O}_3 \gg \text{CH}_3\text{COONa} > \text{EDTA}$ . Only the use of  $0.10 \text{ M Na}_2\text{S}_2\text{O}_3$  solution leads to effective decomplexation of labile  $\text{Ag}(\text{i})$  – calixpyrroles complexes in the membrane. The separation of  $\text{Ag}(\text{i})$  ions from aqueous solutions using  $\text{CH}_3\text{COONa}$  and EDTA was low and did not exceed the value  $\text{RF} = 12\%$ . Maming *et al.*<sup>30</sup> also suggests a  $\text{Na}_2\text{S}_2\text{O}_3$  solution as an appropriate receiving phase in the membrane systems used for the selective  $\text{Ag}(\text{i})$  removal. They demonstrated that PIM containing *p*-tert-butylcalix[4]-arene-tetraethyl ester gives the most efficient transport for  $\text{Ag}(\text{i})$  ions using  $0.10 \text{ M Na}_2\text{S}_2\text{O}_3$  solution as the receiving phase. The recovery factor for  $\text{Ag}(\text{i})$  ions was

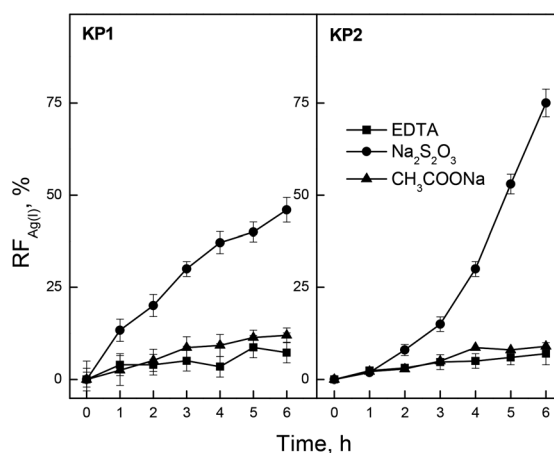


Fig. 6 The recovery factor (RF) obtained for the transport of ions  $\text{Ag}(\text{i})$  across PIM. Source phase:  $5.0 \times 10^{-4} \text{ M AgNO}_3$ ,  $\text{pH} = 4.0$ ; membrane:  $2.0 \text{ cm}^3$  *o*-NPPE/ $1.0 \text{ g}$  CTA;  $0.10 \text{ M}$  **KP1** and **KP2**, receiving phase:  $0.10 \text{ M EDTA}$ ;  $0.10 \text{ M Na}_2\text{S}_2\text{O}_3$  and  $0.10 \text{ M CH}_3\text{COONa}$ . PIMs compositions were 67% plasticizer, 30% support, 3% **KP1**; and 63% plasticizer, 31% support, 6% **KP2**.



65.9%, then. Amiri *et al.*<sup>23</sup> using 0.15 M Na<sub>2</sub>S<sub>2</sub>O<sub>3</sub> as the receiving phase determined the rate and efficiency in the transport of Ag(I) ions through PIM containing calix[4]pyrrole. The flux and RF for Ag(I) were found to be equal to 1.57 μmol m<sup>-2</sup> s<sup>-1</sup>, and 38%, respectively.

### 3.4. An effect of ions carrier concentration

An important factor affecting the efficiency of the separation of metal ions by transport through polymer inclusion membranes is the composition of the membrane phase, *i.e.* the type and concentration of the ion carrier, the type and amount of plasticizer, and the type and thickness of the polymer matrix used. The effect of the type and quantity of the ion carriers derived from calixpyrroles in the polymer inclusion membrane on Ag(I) ions permeation was examined. Membranes with a fixed content of CTA (25 mg) and plasticizer (2 cm<sup>3</sup> *o*-NPPE/1.0 g CTA) were prepared, while the concentration of carrier in the membrane was changed in the range of 0.0010 M to 0.40 M (based on plasticizer volume).

The carrier concentrations in the membranes expressed as percent by weight were for **KP1** 0.05–7% and 0.1–16% for **KP2**.

Each experiment was carried out for 6 hours. The membranes without ion carrier did not transport Ag(I) ions, which indicates that carrier concentration is crucial for the facilitated transport of silver ions through PIM.

The saturation of polymer inclusion membrane with the ion carrier occurs at a concentration equal to 0.10 M (based on plasticizer volume) both for carriers **KP1** and **KP2**. The rate of transport determined for that concentration of the carrier is maximum and reaches 0.71 μmol m<sup>-2</sup> s<sup>-1</sup> for **KP1** and 1.74 μmol m<sup>-2</sup> s<sup>-1</sup> for **KP2**, respectively. Fig. 7 shows the logarithmic plot of the initial flux *versus* the concentration of **KP1** or **KP2** for Ag(I) transport. In the case of PIM containing **KP1**, the flux stabilized at a concentration of 1%, whereas in the case of **KP2**, the flux changed slightly at a carrier concentration of 3%. Exemplary concentration of carrier, CTA and plasticizer in the membrane are shown in the ESI.† Higher values of metal flux

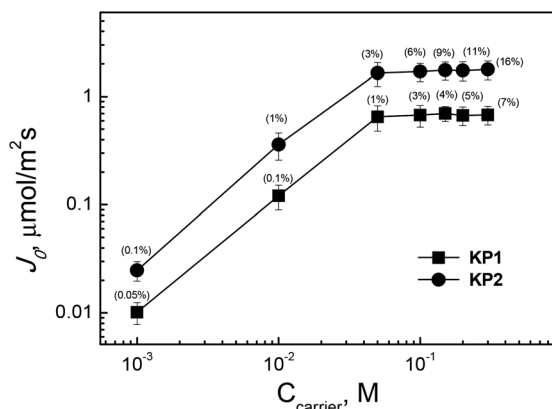


Fig. 7 The Ag(I) transport fluxes vs. ion carrier concentration PIM. Source phase: 1.0 × 10<sup>-3</sup> M AgNO<sub>3</sub>, pH = 4.0; membrane: 2.0 cm<sup>3</sup> *o*-NPPE/1.0 g CTA (carrier concentration expressed in percentage by mass); receiving phase: 0.10 M Na<sub>2</sub>S<sub>2</sub>O<sub>3</sub>.

were observed for CTA-based membranes containing 1% **KP1** and 3% **KP2**, while the content of CTA and *o*-NPPE ranged from 27 to 31% and from 57 to 67%, respectively.

Fig. 8 shows the suggested structure of the complex transported by the liquid phase of the membrane toward the receiving phase where the decomplexing reaction occurs.

The transport of Ag(I) across PIM with **KP2** was faster because formation of a complex in membranes took place *via* both interactions of cations with calixpyrrole *i.e.* *via* cavity ring and the carboxylic group. In the case of **KP1**, additional interaction between the of methylcalixpyrrole group and Ag(I) cation can be neglected and in consequence the formed complex is more labile and the transport of Ag(I) across PIM becomes slower.

The Ag(I) is transported from the source phase to the receiving phase *via* a plasticized membrane. Movement of the Ag(I) through the PIM is possible due to the presence of the carrier. After complexation of the silver and nitrate ion pair with carrier on the left side of the membrane, the complex diffuses down its concentration gradient. On the right side of the membrane, carrier ion pair complex is decomplexed and silver nitrate ion pair is released into the receiving phase. The free carrier diffuses back across the liquid phase in membrane and the cycle is repeated. The net result is the transport of Ag(I) from the aqueous source phase to the aqueous receiving phase across the organic phase in membrane. A similar transport mechanism is described in the papers<sup>31,32</sup> and explained by an increase in the viscosity of organic membrane phase, and thus the resistance of the membrane limiting complex diffusion through the membrane.<sup>31</sup>

### 3.5. An effect of membrane plasticizer

Then, an effect of plasticizer type and its amount in polymer inclusion membranes on Ag(I) transport from source phase at a concentration of 5.0 × 10<sup>-4</sup> M and pH = 4.0 to 0.10 M Na<sub>2</sub>S<sub>2</sub>O<sub>3</sub> solution as receiving phase was examined.

In membrane processes *o*-nitrophenyl pentyl ether (*o*-NPPE), was used as the plasticizer of CTA matrix, which had the same concentration of **KP1** and **KP2** (0.10 M). A series of transport measurements using membrane with a fixed composition of the carrier and matrix (25 mg CTA), plasticizer volume in the range of 0.5–6.0 cm<sup>3</sup> per 1.0 g CTA, was performed for the quantitative determination of the optimum content of *o*-NPPE plasticizer in the membrane (Fig. 9).

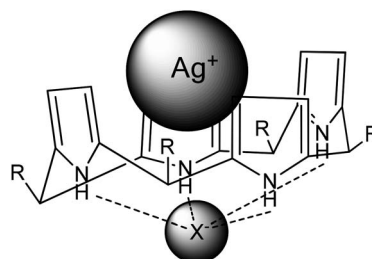


Fig. 8 A suggested silver – calixpyrrole (**KP1** as well as **KP2**) complex transported through a plasticized membrane (X<sup>-</sup> = NO<sub>3</sub><sup>-</sup>).



Introduction of  $4.0 \text{ cm}^3$  or more plasticizer solution per  $1.0 \text{ g}$  CTA did not affect any more the rate of  $\text{Ag}(\text{i})$  transport through PIM. The membrane thickness for optimum conditions, *i.e.*  $4.0 \text{ cm}^3$  *o*-NPPE/ $1.0 \text{ g}$  CTA, was  $25 \text{ }\mu\text{m}$ . The dissolution of calixpyrroles into the matrix was observed in the case of high content of *o*-NPPE ether in polymer inclusion membrane, which resulted in the effective transport of  $\text{Ag}(\text{i})$  ions.  $\text{Ag}(\text{i})$  ions transport was not observed for the non-plasticized CTA membrane with increasing content of the plasticizer used in the membrane to  $4 \text{ cm}^3/1 \text{ g}$  CTA in the case of *o*-NPPE and *o*-NPOE plasticizers (76% and 77 wt%), the permeability of  $\text{Ag}(\text{i})$  ions through PIM increased significantly, and then began to stabilize. In the context of these results it should be noted that Raut *et al.*<sup>33</sup> obtained the maximum permeability of cesium(i) ions for CTA membranes containing calix[4]bis-2,3-naphtho-crown-6 and 65% wt *o*-NPOE. Similar results were presented in the Kaya *et al.*<sup>34</sup> study on the effect of plasticizers for the removal of  $\text{Cr}(\text{iv})$  using calixarenes in plating bath water. They reported that *o*-NPPE was the best plasticizer. Using it the best transport efficiency, with recovery of 98%, was achieved. This was expected because *o*-NPPE has the lowest viscosity and the highest dielectric constant among plasticizer studied.

### 3.6. An effect of polymer matrix

The study on  $\text{Ag}(\text{i})$  ions transport from  $5.0 \times 10^{-4} \text{ M}$   $\text{AgNO}_3$  solution through membranes containing  $0.10 \text{ M}$  **KP1** and **KP2** as ions carriers, as well as cellulose triacetate (CTA) and polyvinyl chloride (PVC) as the matrix, was conducted in order to examine an effect of matrix type in polymer inclusion membrane.

$J_i$  values listed in Table 1 indicate that, compared to PIM with PVC matrix,  $\text{Ag}(\text{i})$  ions are definitely faster transported through polymer inclusion membranes with CTA matrix. This results from the fact that cellulose triacetate membranes are characterized by stronger hydrophilic properties compared to polyvinyl chloride membranes. This induces the need to provide

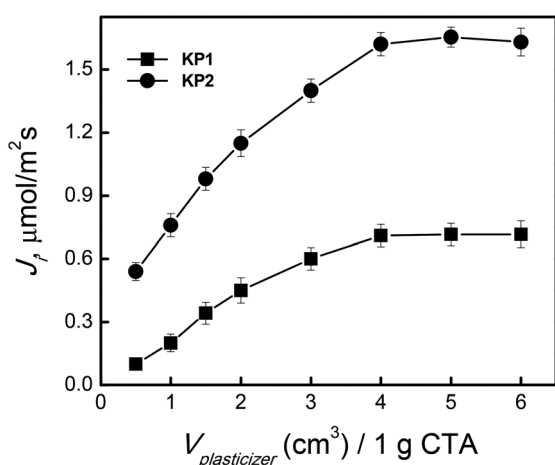


Fig. 9 The effect of *o*-NPPE plasticizer on the  $\text{Ag}(\text{i})$  transport through PIM. Source phase:  $5.0 \times 10^{-4} \text{ M}$   $\text{AgNO}_3$ , pH = 4.0; membrane: 25.0 mg CTA; 0.10 M **KP1** and **KP2**, receiving phase: 0.10 M  $\text{Na}_2\text{S}_2\text{O}_3$ .

more ion carriers. Therefore there is a need to increase the share of plasticizer in the membrane with PVC matrix in order to create the inclusion of the organic phase in the membrane of suitable high dispersion degree, *i.e.* porosity.

CTA-based membranes are more hydrophilic than membranes containing PVC matrix. CTA-based membranes have more expanded and rough surface that allows a better accessibility of the metal ions to the membrane. PVC-based PIMs were more hydrophobic and completely amorphous, and their surface showed less diversity, resulting in worse accessibility.<sup>35</sup>

### 3.7. Separation of $\text{Cu}(\text{ii})$ , $\text{Zn}(\text{ii})$ , $\text{Ag}(\text{i})$ and $\text{Cd}(\text{ii})$ ions

Next stage of the study involved determination of separating ability of calixpyrrole carriers used in transport of metal ions from the source phase containing  $5.0 \times 10^{-4} \text{ M}$  solution of mixture nitrates of  $\text{Ag}(\text{i})$  and  $\text{Cu}(\text{ii})$ ;  $\text{Ag}(\text{i})$  and  $\text{Zn}(\text{ii})$ ;  $\text{Ag}(\text{i})$  and  $\text{Cd}(\text{ii})$ ; at pH 4.0. PIM containing 0.10 M **KP1** or **KP2** and  $4 \text{ cm}^3$  of *o*-NPPE/ $1.0 \text{ g}$  CTA, were applied in those experiments.

Fig. 10 presents the values of recovery factor (RF) as a function of time during a competitive transport of  $\text{Ag}(\text{i})$  and  $\text{Cu}(\text{ii})$  ions. The selectivity of these membrane systems determined by  $\text{Ag}(\text{i}) > \text{Cu}(\text{ii})$  order was the highest for PIM containing **KP2**. After 24 hours, the RF values determined for: **KP2** were 98.9% for  $\text{Ag}(\text{i})$  and 7.2% for  $\text{Cu}(\text{ii})$ ; **KP1** were 80.1% for  $\text{Ag}(\text{i})$  and 7.1% for  $\text{Cu}(\text{ii})$ , respectively. The values of selectivity coefficients are presented in Table 2. They were high due to low affinity of calixpyrroles to  $\text{Cu}(\text{ii})$ .

Studies devoted to the separation ions of  $\text{Ag}(\text{i})$  and  $\text{Cd}(\text{ii})$  across PIM were also performed. It was found that the transport efficiency of these systems was high for  $\text{Ag}(\text{i})$  and very low for  $\text{Cd}(\text{ii})$ . The separation properties of the membranes relative to the ion  $\text{Ag}(\text{i})$  and  $\text{Zn}(\text{ii})$  were also checked. After 24 hours, the RF values determined for **KP1** and **KP2** were 93.66% and 79.45% for  $\text{Ag}(\text{i})$ , respectively. Transport of  $\text{Cu}(\text{ii})$  and  $\text{Zn}(\text{ii})$ ;  $\text{Cu}(\text{ii})$  and  $\text{Cd}(\text{ii})$ , as well as  $\text{Zn}(\text{ii})$  and  $\text{Cd}(\text{ii})$  ions was very slow, and the recovery factor (RF) after 24 hours of the process did not exceed 1%.

Also the selectivity of  $\text{Ag}(\text{i})$ ,  $\text{Cu}(\text{ii})$ ,  $\text{Cd}(\text{ii})$  and  $\text{Zn}(\text{ii})$  ions transport from an equimolar mixture with a concentration of  $5.0 \times 10^{-4} \text{ M}$ , each through PIM containing **KP1** and **KP2**, was examined in the last stage. The receiving phase was 0.10 M  $\text{Na}_2\text{S}_2\text{O}_3$ . Mixtures of metal ions were transported through the

Table 1 The initial flux values for  $\text{Ag}(\text{i})$  transport through PIM containing CTA and PVC as membrane support. Source phase:  $5.0 \times 10^{-4} \text{ M}$   $\text{AgNO}_3$ ; membrane:  $4.0 \text{ cm}^3$  *o*-NPPE/ $1.0 \text{ g}$  CTA; 0.10 M **KP1** and **KP2**; receiving phase: 0.10 M  $\text{Na}_2\text{S}_2\text{O}_3$

| Carrier    | Initial flux, $J_i$ [ $\mu\text{mol m}^{-2} \text{ s}^{-1}$ ] |                 |
|------------|---|-----------------|
|            | CTA   | PVC             |
| <b>KP1</b> | $0.81 \pm 0.10^a$   | $0.57 \pm 0.09$ |
| <b>KP2</b> | $1.86 \pm 0.06$   | $1.30 \pm 0.05$ |

<sup>a</sup> Standard error.



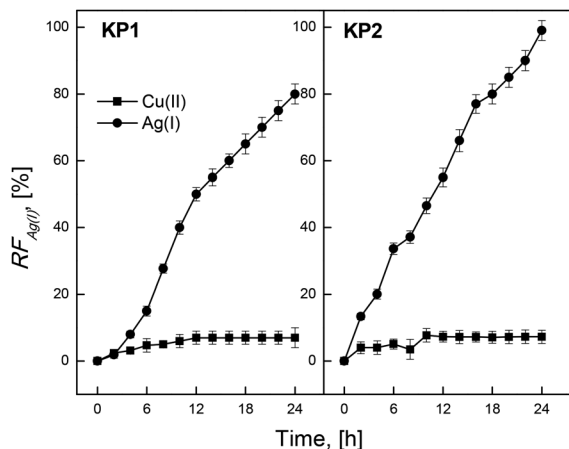


Fig. 10 The relationship of recovery factor (RF) of Ag(I) and Cu(II) vs. time of the transport through PIM. Source phase:  $5.0 \times 10^{-4}$  M AgNO<sub>3</sub> and Cu(NO<sub>3</sub>)<sub>2</sub>, pH = 4.0; membrane: 4.0 cm<sup>3</sup> *o*-NPPE/1.0 g CTA; 0.10 M KP1 and KP2, receiving phase: 0.10 M Na<sub>2</sub>S<sub>2</sub>O<sub>3</sub>.

membranes for 24 hours, and the values of the fluxes from the competitive transport of Ag(I), Cu(II), Cd(II) and Zn(II) were calculated.

Membrane containing KP2 appeared to be effectively separating Ag(I) ions, other metals were separated much more slowly from the aqueous phase, and their initial fluxes did not exceed the value of  $0.10 \mu\text{mol m}^{-2} \text{s}^{-1}$ . The speed of Ag(I) ions transport by these membrane systems is higher for KP2 in comparison with KP1.

### 3.8. Stability of polymer inclusion membranes and supported liquid membranes

An important factor determining the commercial use of polymer inclusion membranes with calixpyrrole carriers is the stability of their operation. Although PIM membranes are considered to be more stable compared to SLM, elution of the carrier from the organic phase and filling the PIM matrix pores has been observed under certain conditions of metal ions transport. This reduces the rate of separation of the studied metal ions.<sup>9</sup> Therefore, it seems appropriate to determine the

stability of PIM containing calixpyrrole carriers and to compare it with the stability of SLM type membranes.

The study on the Ag(I) ions transport in seven measurement cycles (24 hours each) using the same membrane containing 4.0 cm<sup>3</sup> *o*-NPPE/1.0 g CTA as well as 0.10 M KP1 and KP2 in the successive cycles, was performed in order to determine the stability of PIM containing calixpyrrole carriers. The selection of PIM composition allowed to obtain SLM membranes of Celgard 2500 type with identical concentrations of KP1 and KP2 as in PIM. Determination of membrane thickness was for PIM and SLM 25  $\mu\text{m}$ .

The values of Ag(I) ions transport fluxes through PIM determined in subsequent measurements were used to estimate the stability of these membranes.

Determined values of the fluxes in successive measurement cycles decreased insignificantly during the transport through PIM containing KP1 and KP2 (Fig. 11). A noticeable decrease in the fluxes of Ag(I) ions transport in case of PIM with KP2 carrier occurred after the fifth measurement cycle, which can be caused by the tendency to form metal salts on the surface of the membrane. Other carriers demonstrated high stability of the transport, and rate changes varied within the range of their standard deviations.<sup>9</sup>

Similarly, long-term stability measurements were carried out for SLM membranes (Celgard 2500), using the carriers at the same concentration (0.10 M) like in PIM, and *o*-NPPE solvent – Fig. 12.

The results of long-term transport of Ag(I) ions through SLM (Fig. 12) indicate that the membranes containing the examined calixpyrroles were characterized by a decrease in transport fluxes after 96 hours of the process. All examined membrane systems demonstrated the loss in their stability, which resulted in a rapid reduction in the transport rate after four days of the process.

The possible degradation of surface and the sludge which occurred after the Ag(I) ions transport process (Table 3) were supported by scanning electron microscope (SEM) were analyzed.

The comparison of surface microstructure demonstrates the differentiation in membrane matrix materials in terms of

Table 2 Initial flux ( $J_i$ ) and selectivity coefficient ( $S_{M1/M2}$ ) values for Ag(I), Cu(II), Zn(II) and Cd(II). Source phase:  $5.0 \times 10^{-4}$  M each metal nitrate (AgNO<sub>3</sub>; Cu(NO<sub>3</sub>)<sub>2</sub>; Cd(NO<sub>3</sub>)<sub>2</sub>; Zn(NO<sub>3</sub>)<sub>2</sub>); membrane: 4.0 cm<sup>3</sup> *o*-NPPE/1.0 g CTA; 0.10 M KP1 and KP2; receiving phase: 0.10 M Na<sub>2</sub>S<sub>2</sub>O<sub>3</sub>

| Carrier | Metal ions | Initial flux, $J_i$ [ $\mu\text{mol m}^{-2} \text{s}^{-1}$ ] | Selectivity coefficient, $S_{M1/M2}$    |
|---------|------------|--|---|
| KP1     | Ag(I)      | 0.70   | $S_{\text{Ag(I)}/\text{Cu(II)}} = 10.3$ |
|         | Cu(II)     | 0.07   |   |
|         | Ag(I)      | 0.70   | $S_{\text{Ag(I)}/\text{Cd(II)}} = 15.6$ |
|         | Cd(II)     | 0.05   |   |
|         | Ag(I)      | 0.70   | $S_{\text{Ag(I)}/\text{Zn(II)}} = 20.0$ |
| Zn(II)  | 0.04       |  |   |
| KP2     | Ag(I)      | 1.60   | $S_{\text{Ag(I)}/\text{Cu(II)}} = 16.0$ |
|         | Cu(II)     | 0.10   |   |
|         | Ag(I)      | 1.60   | $S_{\text{Ag(I)}/\text{Cd(II)}} = 53.3$ |
|         | Cd(II)     | 0.03   |   |
|         | Ag(I)      | 1.60   | $S_{\text{Ag(I)}/\text{Zn(II)}} = 80.0$ |
| Zn(II)  | 0.02       |  |   |





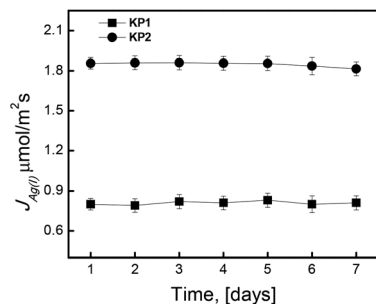


Fig. 11 Changes of the Ag(I) flux during transport across PIM – 7 cycles of measurement. Source phase:  $5.0 \times 10^{-4}$  M AgNO<sub>3</sub>, pH = 4.0; membrane: 4.0 cm<sup>3</sup> *o*-NPPE/1.0 g CTA; 0.10 M KP1 and KP2, receiving phase: 0.10 M Na<sub>2</sub>S<sub>2</sub>O<sub>3</sub>.

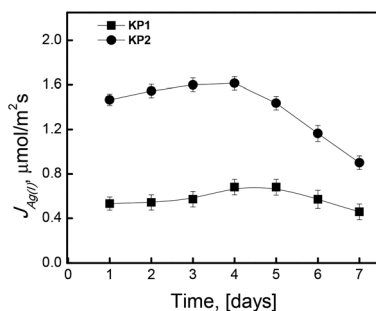


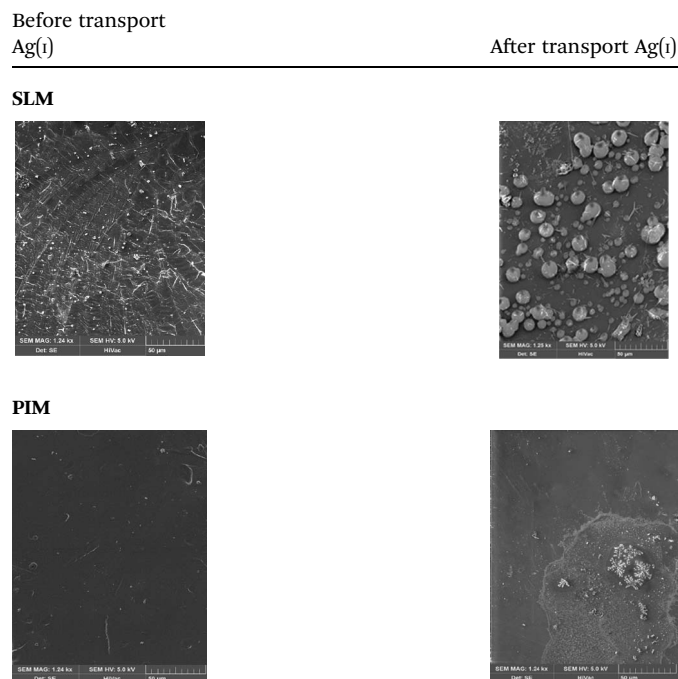
Fig. 12 The flux transport of Ag(I) ions calculated obtained for long-term transport across SLM. Source phase:  $5.0 \times 10^{-4}$  M AgNO<sub>3</sub>, pH = 4.0; membrane: 4.0 cm<sup>3</sup> *o*-NPPE/1.0 g CTA; 0.10 M KP1 and KP2, receiving phase: 0.10 M Na<sub>2</sub>S<sub>2</sub>O<sub>3</sub>.

quantity and sediment distribution as a result of the phenomena of Ag(I) ions accumulation in the membrane phase. They are especially evident in the case of SLM membranes with calixpyrroles **KP2**, as distinct changes in membrane appearance are observed in that case. Crystal structures and sediments which may be metal complexes or carrier were observed in SLM, such only slightly sediments were observed in the PIM membrane, probably caused by insoluble silver salt formation.

### 3.9. PIMs characterization by AFM

Crucial information on the membrane uniformity, roughness, and pore size was obtained by means of AFM. The AFM images of PIM formed with CTA + *o*-NPPE (Fig. 13a) and CTA + *o*-NPPE + **KP1** (Fig. 13b) and CTA + *o*-NPPE + **KP2** (Fig. 13c) were taken in a 3D format of 10 μm × 10 μm. As seen in Fig. 13b, the blank membrane is not porous. The roughness parameters ( $R_a$ ) of the areas for the **KP1** and **KP2** membrane before metal ions transport were 3.64 nm and 4.09 nm, respectively. The ( $R_a$ ) of the PIM **KP1** and **KP2** after metal ions transport were 2.31 nm and 3.37 nm, respectively; this parameter is less than before metal ions transport. This difference can be attributed to the differences between the surface of the blank membrane and PIM due to the inclusion of carrier.

Table 3 SEM images before and after the transport of ions Ag(I) across PIM and SLM containing KP2 (magnification 50 μm)



On all membranes containing **KP1** and **KP2**, well-formed inclusions in the polymer of the matrix containing carrier in the plasticizer solution can be seen. In the case of the polymer

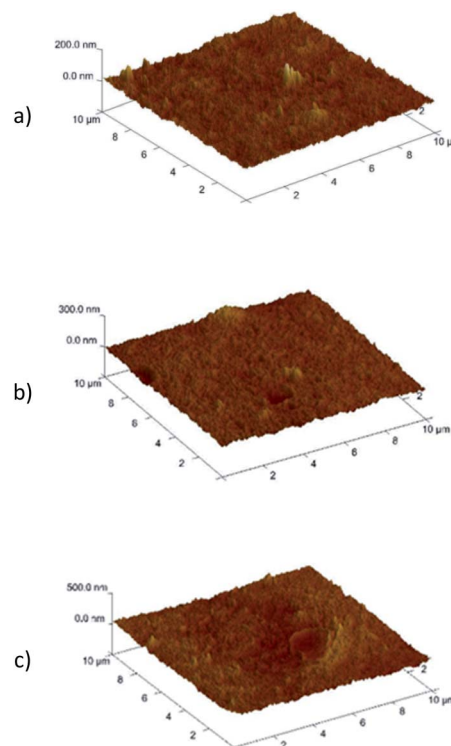


Fig. 13 3D-atomic force microscopy (AFM) images of PIM without carrier (a), PIM containing **KP1** (b) as well as PIM containing **KP2** (c).



inclusion membrane with **KP2**, the inclusions formed have the shape of elongated drops and the “porosity” is about 50%.

## 4 Conclusions

The study of Cu(II), Zn(II), Ag(I) and Cd(II) ions transport through polymer inclusion membranes containing derivatives of calix[4]pyrroles as the carriers of ions allowed to specify the factors determining the rate, efficiency and selectivity of these metal ions transport. It was confirmed that the transport of Ag(I) ions through polymer inclusion membranes follows the model of the first order reaction kinetics for metal ions transport. Investigation on modification of the source phase composition demonstrated that the values of initial Ag(I) ions transport fluxes increase with an increasing pH from 2.0 to 4.0. However, in the pH range 4.0–6.0, transport flux was stabilized and the parameters did not change their values. The study concerning modification of receiving phase composition showed that 0.10 M Na<sub>2</sub>S<sub>2</sub>O<sub>3</sub> solution proved to be an effective reagent in decomplexation of labile Ag(I) – calixpyrroles complex in the membrane. Among the examined plasticizers, *o*-nitrophenyl pentyl ether (*o*-NPPE) proved to be the suitable plasticizer for the membranes containing calixpyrroles carriers, and permeability of these membranes with respect to the examined ions increases with an increasing concentration of that plasticizer, and reaches the maximum value for membranes containing 4.0 cm<sup>3</sup> of *o*-NPPE/1.0 g CTA. Polyvinyl chloride is a less efficient support in the polymer inclusion membrane than cellulose triacetate, which results in lower values of Ag(I) ions transport flux. A comparison of Ag(I) ions transport through polymer inclusion membranes and supported liquid membranes (Celgard 2500) showed much higher stability of the first membrane, which allows their multiple use. High values of coefficients of Ag(I) ions separation with respect to the other metals (Cu(II), Zn(II), Cd(II)) proved the selectivity of the examined membrane, which in turn was related to the low affinity of calixpyrrole molecules with respect to divalent cations.

By the use of microscopic methods and in particular atomic force microscopy, it was shown that the membrane of CTA and plasticizer itself is not porous and only slightly corrugated due to the different rate of evaporation of the solvent. On all membranes containing **KP1** and **KP2** one can see well-formed inclusions in the matrix polymer containing a carrier in plasticizer solution. In the case of the polymer inclusion membrane with **KP2**, the inclusions of liquid organic phase formed into CTA have the shape of elongated drops and the porosity is about 50%.

## Conflicts of interest

The authors declare no conflict of interest.

## Acknowledgements

This research was funded by the National Science Center funds allocated on the basis of the decision number DEC-2013/09/N/ST5/02984.

## References

- 1 D. Wang, J. Hu, D. Liu, Q. Chen and J. Li, *J. Membr. Sci.*, 2017, **524**, 205.
- 2 F. Kubota and M. Goto, *Solvent Extr. Res. Dev.*, 2006, **13**, 23.
- 3 L. Nghiem, P. Mornane, I. Potter, J. Perera, R. Cattrall and S. Kolev, *J. Membr. Sci.*, 2008, **281**, 7.
- 4 M. I. G. S. Almeida, R. W. Cattrall and S. D. Kolev, *J. Membr. Sci.*, 2012, **415–416**, 9.
- 5 C. Onaca, A. Kayaa, M. Lütfi Yolab and H. K. Alpoguz, *ECS J. Solid State Sci. Technol.*, 2017, **6**, M152–M155.
- 6 C. Onac, A. Kaya, I. Sener and H. K. Alpoguz, *J. Electrochem. Soc.*, 2018, **165**(2), E76–E80.
- 7 A. M. Sastre, A. Kumar, J. P. Shukla and R. K. Singh, *Sep. Purif. Methods*, 1998, **27**, 213.
- 8 M. Aguilar, and J. L. Cortina, *Solvent Extraction and Liquid Membranes–Fundamentals and Applications in New Materials*, CRC Press Taylor & Francis Group, Boca Raton 2008.
- 9 A. Y. Nazarenko and J. D. Lamb, *J. Inclusion Phenom.*, 1997, **29**, 247.
- 10 D. Wang, R. W. Cattrall, J. Li, M. I. G. S. Almeida, G. W. Stevens and S. D. Kolev, *J. Membr. Sci.*, 2017, **542**, 272.
- 11 S. Kagaya, Y. Ryokan, R. W. Cattrall and S. D. Kolev, *Sep. Purif. Technol.*, 2012, **101**, 69.
- 12 W. Yoshida, Y. Baba, F. Kubota, S. D. Kolev and M. Goto, *J. Membr. Sci.*, 2019, **572**, 291.
- 13 P. A. Gale, J. L. Sessler and V. Král, Calixpyrroles, *Chem. Commun.*, 1998, (1), 1.
- 14 M. I. G. S. Almeida, R. W. Cattrall and S. D. Kolev, *Anal. Chim. Acta*, 2017, **987**, 1.
- 15 K. Annane, A. Sahmoune, P. Montels and S. Tingry, *Chem. Eng. Res. Des.*, 2015, **94**, 605.
- 16 P. Pantuckova, P. Kuban and P. Bocek, *Anal. Chim. Acta*, 2015, **887**, 111.
- 17 I. Perez-Silva, J. A. Rodríguez, M. T. Ramírez-Silva and M. E. Paez-Hernandez, *Anal. Chim. Acta*, 2012, **718**, 42.
- 18 A. Gale, J. L. Sessler, V. A. Král and V. Lynch, *J. Am. Chem. Soc.*, 1996, **118**, 5140.
- 19 M. S. Alam, K. Inoue, Y. Yoshizuka, Y. Dong and P. Zang, *Hydrometallurgy*, 1997, **44**, 245.
- 20 Z. Hubicki and H. Hubicka, *Hydrometallurgy*, 1995, **37**, 207.
- 21 A. Gherrou and H. Kerdjoudj, *Desalination*, 2002, **151**, 87.
- 22 A. Nowik-Zajac, C. Kozłowski and A. Trochimczuk, *Desalination*, 2012, **94**, 25.
- 23 A. A. Amiri, A. Safavi, A. R. Hasaninejad, H. Shrghi and M. Shamsipur, *J. Membr. Sci.*, 2008, **325**, 295.
- 24 M. Shamsipur, S. Y. Kazemi, G. Azimi, S. S. Madaeni, V. Lippolis, A. Garau and F. Isaia, *J. Membr. Sci.*, 2003, **215**, 87.
- 25 J. Maming, D. Siswanta and H. Sastrohamidojojo, *Indones. J. Chem.*, 2007, **7**, 172.
- 26 P. Anzenbacher Jr, K. Jursíková, V. M. Lynch, P. A. Gale and J. L. Sessler, *J. Am. Chem. Soc.*, 1999, **121**, 11020.
- 27 P. R. Danesi, *Sep. Sci. Technol.*, 1984–85, **19**, 857.



- 28 S. Tarahomi, G. H. Rounaghi, H. Eshghi, L. Daneshvar and M. Chamsaz, *J. Braz. Chem. Soc.*, 2017, **28**, 68.
- 29 M. Shamsipur, S. Y. Kazemi, G. Azimi, S. S. Madaeni, V. Lippolis, A. Garau and F. Isaia, *J. Membr. Sci.*, 2003, **215**, 87.
- 30 J. Maming, D. Siswanta, H. Firdaus and H. Sastrohamidojojo, *Indones. J. Chem.*, 2008, **8**, 72.
- 31 R. D. Noble, Generalized Microscopic Mechanism of Facilitated, *J. Membr. Sci.*, 1992, **75**, 121.
- 32 O. Arous, H. Kerdjoudj and P. Seta, *J. Membr. Sci.*, 2004, **241**, 177.
- 33 D. R. Raut, P. Kandwal, G. Rebello and P. K. Mohapatra, *J. Membr. Sci.*, 2012, **407–408**, 17.
- 34 A. Kaya, C. Onac, H. K. Alpoguz, A. Yilmaz and N. Atar, *Chem. Eng. J.*, 2016, **283**, 141.
- 35 M. Baczynska, M. Waszak, M. Nowicki, D. Prządka, S. Borysiak and M. Regel-Rosocka, *Ind. Eng. Chem. Res.*, 2018, **57**, 5070.

